

Targeted Cargo Delivery in Senescent Cells Using Capped Mesoporous Silica Nanoparticles**

Alessandro Agostini, Laura Mondragón, Andrea Bernardos, Ramón Martínez-Máñez,*
M. Dolores Marcos, Félix Sancenón, Juan Soto, Ana Costero, Cristina Manguan-García,
Rosario Perona,* Marta Moreno-Torres, Rafael Aparicio-Sanchis, and José Ramón Murguía*

Normal somatic cells invariably enter a state of irreversibly arrested growth and altered function after a finite number of divisions, called cellular senescence. Senescent cells display a radically altered phenotype that is thought to impair tissue function and predispose tissues to disease development and/or progression. Despite the fact that the immune system destroys many senescent cells, it becomes much less effective at this task during aging. As a consequence, senescent or “death resistant” cells accumulate in tissues, thus accelerating aging and contributing to disease development. Senescent-cell accumulation alters neighboring cell behavior, favors degradation of the extracellular matrix, decreases the pool of mitotic-competent cells, and stimulates cancer.^[1] Moreover

a number of pathologies are associated with accelerated cellular aging such as Werner adult progeria syndrome (WS), Hutchinson–Gilford syndrome (HGS), and Rothmund–Thompson syndrome (RTS).^[2] In WS or RTS, the shortening of telomeres is observed in most tissues, even if defective telomerase is not the main cause of the disease.^[3,4] Other diseases are more related to tissue-specific accelerated aging such as Dyskeratosis congenita (DC) and idiopathic pulmonary fibrosis (IPF).^[5] In these conditions, the replicative capacity of cells is impaired by defective telomerase activity in the stem-cell compartment of high turnover tissues such as skin, pulmonary epithelium, and bone marrow. A frequently associated secondary effect in these diseases is the induction of cancer, especially in those that involve a shortening of the telomeres.^[6] To combat this problem, strategies to prevent, replace, or remove senescent cells are of fundamental interest both for basic research and clinical applications. In particular, the design of such therapies could contribute to the treatment of accelerated cellular-aging diseases and may boost the long-term possibility of human rejuvenation. In fact, as a proof-of-concept, two recent studies supported the fundamental concept that senescent cells can drive the aging process and that their elimination can be therapeutic. First, inducible removal of p16-positive senescent cells in a genetically engineered progeroid-mouse background arrested virtually all of the accelerated aging phenotypes.^[7] Second, tissue degeneration was reversed by reactivation of telomerase expression in aged telomerase-deficient mice.^[8] However, these examples were applied to transgenic mice and effective strategies involving the pharmacological reactivation, removal, or replacement of senescent cells for treating aging-related conditions in human patients are currently unavailable. A first approach to achieve this goal would be to develop selective-delivery carriers that are able to release their cargo in the senescent cells. However, as far as we know, such targeted release systems have not been described.

Nanotechnology has proven to be an innovative approach for drug-delivery therapies. Drug-delivery systems able to release active molecules to certain cells in a controlled manner have recently gained much attention. Microcapsules, polymers,^[9] dendrimers,^[10] micelles,^[11] and nanoparticles^[12] have been used as potential drug-delivery systems. Alternatively, mesoporous silica nanoparticles (MSNs) have been widely used as reservoirs for drug storage^[13] because of their unique mesoporous structure, large specific volume, and easy functionalization. Moreover MSNs are in general biocompatible and have been reported to undergo cellular uptake by

[*] A. Agostini,^[+] Dr. L. Mondragón,^[+] Dr. A. Bernardos, Prof. R. Martínez-Máñez, Dr. M. D. Marcos, Dr. F. Sancenón, Dr. J. Soto
Centro de Reconocimiento Molecular y Desarrollo Tecnológico (IDM), Unidad Mixta Universitat Politècnica de València-Universitat de València. CIBER de Bioingeniería, Biomateriales y Nanomedicina (CIBER-BBN)
Camino de Vera s/n, 46022 Valencia (Spain)
E-mail: rmaez@qim.upv.es

Prof. A. Costero
Centro de Reconocimiento Molecular y Desarrollo Tecnológico (IDM), Unidad Mixta Universitat Politècnica de València-Universitat de València. Departamento de Química Orgánica, Facultad de Ciencias Químicas, Universidad de Valencia
Doctor Moliner 50, 46100 Burjassot, Valencia (Spain)


Dr. C. Manguan-García, Prof. R. Perona
Instituto de Investigaciones Biomédicas CSIC/UAM
IDIPaz, Madrid (Spain)

and
CIBER de Enfermedades Raras (CIBERER)
E-mail: rperona@iib.uam.es

Dr. M. Moreno-Torres, Dr. R. Aparicio-Sanchis, Prof. J. R. Murguía
Instituto Universitario Mixto de Biología Molecular y Celular de Plantas
Camino de Vera s/n, 46071 Valencia (Spain)
E-mail: muribajo@ibmcp.upv.es

[+] These authors contributed equally to this work.

[**] We thank the Spanish Government (projects MAT2009-14564-C04 and FIS PI11-0949) the Generalitat Valencia (project PROMETEO/2009/016), and the Universidad Politécnica de Valencia (UPV PAID-05-09) for support. We thank Fundación Ramón Areces for support. C.M.-G. is supported by CIBERER. L.M. thanks the Generalitat Valenciana for her VALI + D postdoctoral contract.

 Supporting information for this article (experimental details) is available on the WWW under <http://dx.doi.org/10.1002/anie.201204663>.

way of endocytosis. Additionally MSNs can be functionalized with molecular/supramolecular ensembles on their external surface to develop gated MSNs showing “zero delivery” (that is, the hybrid material alone is unable to release the payload) and are capable of releasing their cargo in response to external stimuli. Using this concept, MSNs displaying controlled release using several different stimuli have been reported.^[14–25]

Given the need to develop new ways of preventing the appearance of senescence-related human impairment and disease, we present herein the design of nanoparticles that are able to display selective and controlled cargo delivery in senescent cells. Our strategy involves the use of MSNs capped with a galacto-oligosaccharide (GOS) and the presence of senescence associated β -galactosidase (SA- β -gal) specifically in senescent cells. The existence of SA- β -gal in these cells was described in 1995^[26] and its presence explained by the overexpression of the endogenous lysosomal β -galactosidase that specifically occurs in senescent cells.^[27] The source of SA- β -gal activity in senescent cells is encoded by the *GLB1* gene^[27] and its presence is a surrogate marker for increased lysosome number or activity, which has long been associated with replicative senescence^[29,30] and organismal aging.^[31,32] We reasoned that if easily derivatized with GOS, the gated mesoporous nano-devices would show “zero release”, yet would selectively release their cargo senescent cells because of β -galactosidase-mediated hydrolysis of the cap (Figure 1 A).

For this study, MCM-41-based MSNs were selected as the inorganic scaffold.^[33] The structure of the mesoporous starting material was confirmed by X-ray diffraction and TEM (Figure 1 B). For the preparation of the final capped nanodevice (**S1**), the calcined MSNs were first loaded with Rhodamine-B as a model drug and then reacted with the capping oligosaccharide derivative **3** (see Supporting Information). **3** was prepared starting from a commercially available galacto-oligosaccharide polymer (GOS) which was first brought to pH 7.0 and then reacted with 3-aminopropyltriethoxysilane to give the corresponding alkylgluconamine derivative (see Supporting Information for details).^[34] The mesoporous structure of **S1** was confirmed by XRD and TEM studies. The final nanoparticles were roughly spherical having a diameter of approximately 100 nm and an average pore diameter of 2.5 nm (Figure 1 B). The N_2 adsorption-desorption isotherm of **S1** (see Supporting Information) was typical of mesoporous systems with capped mesopores, and a significant decrease in the N_2 volume adsorbed and surface area ($228.4 \text{ m}^2 \text{ g}^{-1}$) was observed when compared with the starting MCM-41-based MSNs ($999.6 \text{ m}^2 \text{ g}^{-1}$). The maximum loading of the Rhodamine-B dye from the final material **S1** amounted to 0.14 grams per gram SiO_2 . More-

over the content of the anchored **3** in **S1** amounted to 0.28 grams per gram SiO_2 .

In vitro studies of the delivery of the Rhodamine-B cargo from the MSN **S1** in water in the presence and absence of β -gal were performed (Figure 1 C). The amount of dye released was determined by monitoring the emission of the Rhodamine-B in the solution as a function of time ($\lambda_{\text{ex}} = 550 \text{ nm}$, $\lambda_{\text{em}} = 580 \text{ nm}$). In the absence of the enzyme β -gal a flat baseline was found indicating that the Rhodamine-B cargo remained in the nanoparticles without release. In contrast, in the presence of β -gal, release of the Rhodamine-B was shown as an increase of the dye fluorescence as a function of time. This behavior was assigned to the galactosidase-induced hydrolysis of the glycosidic bonds of the anchored GOS derivative, which results in a reduction of the size of the attached groups and allows delivery of the entrapped cargo. To confirm this, the supernatant of different aliquots as a function of time of an **S1** and β -gal mixture in water were analyzed by MALDI-TOF-MS spectroscopy. At zero minutes no saccharide fragments were observed, whereas in subsequent aliquots (increasing hydrolysis time) peaks corresponding to the galactose monomer appeared. In parallel, we

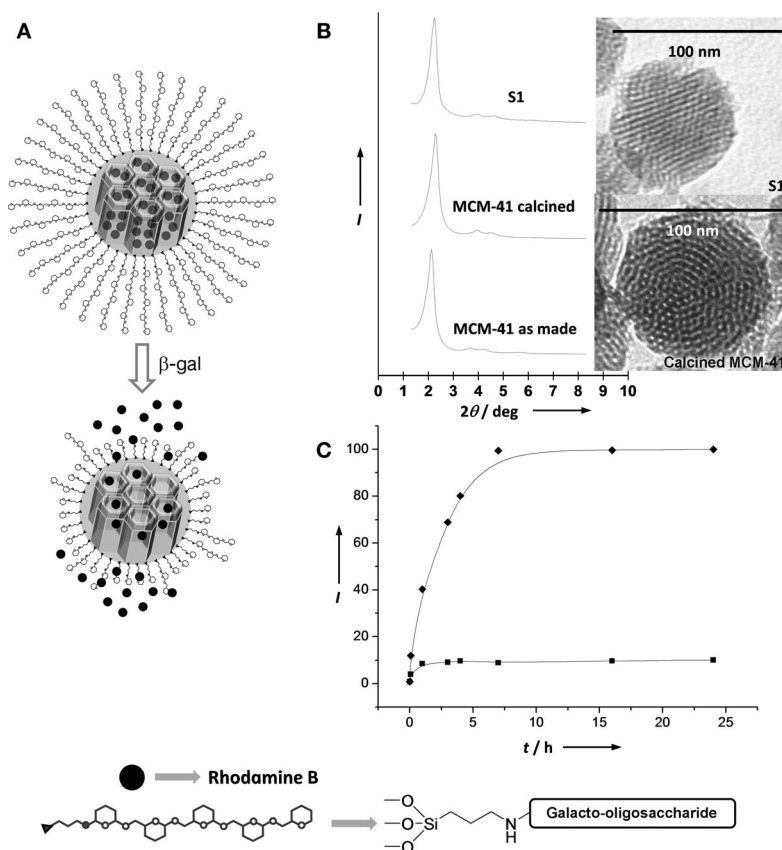


Figure 1. Synthesis and characterization of MSN **S1** nanoparticles. A) Representation of the gated material **S1** capped with a galacto-oligosaccharide (GOS) and the selective delivery mechanism in the presence of β -gal enzyme. B) Powder X-ray diffraction patterns of MCM-41 as synthesized, calcined MCM-41 and the final **S1**. TEM images of calcined MCM-41 and solid **S1** showing the typical porosity of the MCM-41 mesoporous matrix. C) Release profiles of Rhodamine-B dye from MSN **S1** in the absence (\blacksquare) and in the presence (\blacklozenge) of β -gal enzyme in water at pH 7.5 at room temperature.

confirmed that free galactose increased with time using a galactose-detection kit (Deltaclon).

Moreover, to demonstrate that β -gal is responsible for the release observed two additional experiments were performed. In one of them solid **S1** was incubated in the presence of the protease pepsin, whereas in a second experiment the β -gal enzyme was denatured by heating. In both experiments no release of the dye was observed from **S1**. In addition, we also studied the release of the Rhodamine-B dye from **S1** suspended in cellular media and found no dye release in the absence of β -gal.

After demonstrating the effective release of Rhodamine-B from **S1** in the presence of β -gal in vitro, cargo release from **S1** in several in vivo models was studied. First, budding yeast cells were selected because of their genetic tractability and ease of manipulation. Wild-type (WT) and β -gal overexpressing (β -Gal^{oe}) yeast cells were incubated with MSN **S1** nanoparticles and examined for Rhodamine-B staining by fluorescence microscopy. Staining was only detected in β -Gal^{oe} yeast cells with high β -gal activity (Figure 2A,B). Moreover, incubation with MSN **S1** nanoparticles did not affect cell viability throughout the whole experiment (see Supporting Information).

We extended our study to the potential applicability of these GOS-capped MSNs in human senescent cells. As model cells, we used fibroblasts from X-linked Dyskeratosis Congenita (X-DC) patients. X-DC is an inherited rare disease that originates through defects in the telomere maintenance machinery, resulting in shortened telomeres in high-turnover tissues such as bone marrow and skin. Mutations in the *DKC1* gene, encoding a 58 kD nucleolar protein that is associated with small nucleolar RNAs (snoRNAs) in the H/ACA snoRNP (small nucleolar ribonucleoprotein) complexes, are responsible for X-DC.^[35] We used the cell lines X-DC1774 and X-DC4646 containing the c.109_111delCTT and c.385 A > T mutations in *DKC1*, respectively. Aged control human fibroblasts DC1787 and H460 non-small-cell lung-cancer (NSCLC) cells expressing telomerase were also used. X-DC1774, X-DC4646, and aged control fibroblasts DC1787, but not H460 cells, expressed SA- β -gal (Figure 2C). These cell lines were incubated with Rhodamine-loaded MSN **S1** and monitored by time-lapse microscopy (Figure 2D). The Rhodamine released from the particles began at three hours and lasted at least until two days. Remarkably, only X-DC1774, X-DC4646, and DC1787 SA- β -gal positive cells exhibited fluorescence. No emission was detected in H460 cells even after 48 hours. Furthermore, cell viability remained unaffected in H460 and DC-1787 cells, for up to 48 hours incubation with Rhodamine-loaded MSN **S1** (see Supporting Information). Viability results were in good

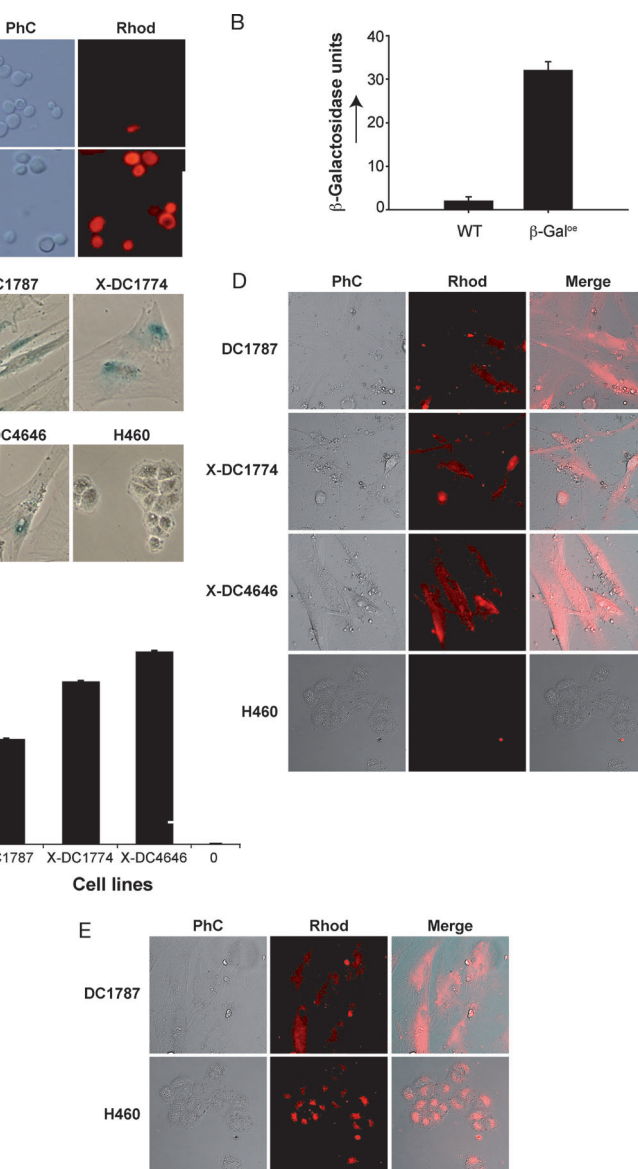


Figure 2. Internalization and release of cargo in β -gal overexpressing (β -Gal^{oe}) yeast cells and human senescent cells. A) Controlled release of Rhodamine-loaded **S1** nanoparticles in wild-type (WT) and β -galactosidase overexpressing (β -Gal^{oe}) yeast cells. Exponentially growing yeast cultures were incubated with **S1** nanoparticles and examined for Rhodamine staining (Rhod) by fluorescence microscopy (right) and Nomarski optics (left). B) Quantitation of β -galactosidase activity in WT and β -Gal^{oe} yeast cells. Data represent the mean \pm standard error of at least three independent experiments, each done in duplicate. Three independent β -Gal^{oe} strains from the same transformation were assayed with essentially identical results. C) DC1787, X-DC 1774, and X-DC4646 human senescent cells and H460 NSCLC cells were grown in 6-well plates and fixed after four days to assay the acid- β -galactosidase activity. Graph shows the quantitation of the percentage of blue cells (β -gal positive) of the total cell population. D) Cells described in (C) were seeded onto μ -slide 8-well ibiTreat microscopy chambers and treated with 50 $\mu\text{g mL}^{-1}$ MSN **S1** Rhodamine-loaded particles. Representative images at 24 h from phase contrast (PhC), Rhodamine (Rhod), and combined (Merge) are shown. E) DC1787 and H460 cells were seeded as in (D) and treated with silica mesoporous support particles anchored with starch. Images were taken and processed as in (D). Representative images at 24 h are shown.

agreement with the observation that in general MSNs exhibit good biocompatibility.^[36] Moreover, although some reports

suggested that, depending on the route of administration in vivo, MSNs might become toxic,^[37] our own data in human cells, are encouraging from the perspective of the potential use of **S1** in in vivo models.

The experiments shown above clearly and remarkably show that despite the fact that GOS-capped **S1** nanoparticles are internalized in all cell types studied, they only released their cargo in β -gal overexpressing cells. Additionally, to demonstrate that the lack of Rhodamine staining in H460 cells was not an artifact of the conditions used, additional control experiments were performed. Rhodamine-loaded MSN nanoparticles capped with hydrolyzed starch were prepared (solid **S2**). MSNs of **S2** are similar to **S1** but contain an oligosaccharide that is hydrolyzed by the amylase enzyme in lysosomes.^[38] When using **S2** in internalization studies under similar conditions to those described above, clearly detectable staining was observed in both of the cell lines studied (Figure 2E), indicating that the release of Rhodamine from **S1** can be ascribed to a selective cellular β -gal enzyme-mediated mechanism.

In summary, the MSN **S1** nanoparticles described herein have proven to be suitable nanodevices to selectively release their cargo in senescent cells with high specificity and a lack of detectable toxicity. Nanoparticles **S1** were able to selectively deliver their cargo in SA- β -gal positive β -Gal^{oe} yeast cells, in aged human fibroblasts DC1787, and in X-DC1774 and X-DC4646 cells from human Dyskeratosis Congenita patients, whereas no cargo release from **S1** was observed in control experiments with H460 non-small-cell lung-cancer cells and wild-type yeast cells. To our knowledge, this is the first time that a nanotherapy has been targeted to senescent cells. These results suggest that by choosing an appropriate cargo (that is a telomerase reactivation drug or a cytotoxic drug) prevention and removal/replacement of senescent cells could be possible. Despite the fact that the road from these results to senescent-cell removal or rejuvenation therapies remains long and uncertain, we believe that our findings might open up new avenues for developing innovative therapeutic applications to treat or delay age-related diseases.

Received: June 14, 2012

Revised: July 31, 2012

Published online: September 20, 2012

Keywords: controlled release · drug delivery · dyskeratosis congenita · gated mesoporous materials · nanoparticles

- [1] D. G. Burton, *Cellular senescence, ageing and disease*, Vol. 31, Age, Dordrecht, Netherlands, **2009**, pp. 1–9.
- [2] C. R. Burtner, B. K. Kennedy, *Nat. Rev.* **2010**, *11*, 567–578.
- [3] N. Ishikawa, K. Nakamura, N. Izumiya-Shimomura, J. Aida, A. Ishii, M. Goto, Y. Ishikawa, R. Asaka, M. Matsuura, A. Hatamochi, M. Kuroiwa, K. Takubo, *Aging* **2011**, *3*, 417–429.
- [4] A. K. Ghosh, M. L. Rossi, D. K. Singh, C. Dunn, M. Ramamoorthy, D. L. Croteau, Y. Liu, V. A. Bohr, *J. Biol. Chem.* **2012**, *287*, 196–209.
- [5] R. T. Calado, N. S. Young, *N. Engl. J. Med.* **2009**, *361*, 2353–2365.
- [6] B. P. Alter, N. Giri, S. A. Savage, P. S. Rosenberg, *Blood* **2009**, *113*, 6549–6557.
- [7] D. J. Baker, T. Wijshake, T. Tchkonja, N. K. LeBrasseur, B. G. Childs, B. van de Sluis, J. L. Kirkland, J. M. van Deursen, *Nature* **2011**, *479*, 232–236.
- [8] M. Jaskelioff, F. L. Muller, J. H. Paik, E. Thomas, S. Jiang, A. C. Adams, E. Sahin, M. Kost-Alimova, A. Protopopov, J. Cadiñanos, J. W. Horner, E. Maratos-Flier, R. A. DePinho, *Nature* **2011**, *469*, 102–106.
- [9] S. Liu, R. Maheshwari, K. L. Kiick, *Macromolecules* **2009**, *42*, 3–13.
- [10] C. C. Lee, J. A. MacKay, J. M. Frechet, F. C. Szoka, *Nat. Biotechnol.* **2005**, *23*, 1517–1526.
- [11] C. W. Pouton, C. J. Porter, *Adv. Drug Delivery Rev.* **2008**, *60*, 625–637.
- [12] I. Brigger, C. Dubernet, P. Couvreur, *Adv. Drug Delivery Rev.* **2002**, *54*, 631–651.
- [13] M. Vallet-Regí, F. Balas, D. Arcos, *Angew. Chem.* **2007**, *119*, 7692–7703; *Angew. Chem. Int. Ed.* **2007**, *46*, 7548–7558.
- [14] T. D. Nguyen, K. C. F. Leung, M. Liong, Y. Liu, J. F. Stoddart, J. I. Zink, *Adv. Funct. Mater.* **2007**, *17*, 2101–2110.
- [15] B. G. Trewyn, S. Giri, I. I. Slowing, V. S. Y. Lin, *Chem. Commun.* **2007**, 3236–3245.
- [16] R. Klajn, J. F. Stoddart, B. A. Grzybowski, *Chem. Soc. Rev.* **2010**, *39*, 2203–2237.
- [17] E. Climent, A. Bernardos, R. Martínez-Mañez, A. Maquieira, M. D. Marcos, N. Pastor-Navarro, R. Puchades, F. Sancenón, J. Soto, P. Amorós, *J. Am. Chem. Soc.* **2009**, *131*, 14075–14080.
- [18] A. Schlossbauer, J. Kecht, T. Bein, *Angew. Chem.* **2009**, *121*, 3138–3141; *Angew. Chem. Int. Ed.* **2009**, *48*, 3092–3095.
- [19] B. G. Trewyn, I. I. Slowing, S. Giri, H. T. Chen, V. S. Y. Lin, *Acc. Chem. Res.* **2007**, *40*, 846–853.
- [20] S. Saha, K. C. F. Leung, T. D. Nguyen, J. F. Stoddart, J. I. Zink, *Adv. Funct. Mater.* **2007**, *17*, 685–693.
- [21] Y.-W. Yang, *Med. Chem. Commun.* **2011**, *2*, 1033–1049.
- [22] a) E. Climent, R. Martínez-Mañez, F. Sancenón, M. D. Marcos, J. Soto, A. Maquieira, P. Amorós, *Angew. Chem.* **2010**, *122*, 7439–7441; *Angew. Chem. Int. Ed.* **2010**, *49*, 7281–7283; b) A. Agostini, L. Mondragón, C. Coll, E. Aznar, M. D. Marcos, R. Martínez-Mañez, F. Sancenón, J. Soto, E. Pérez-Payá, P. Amorós, *ChemistryOpen* **2012**, *1*, 17–20.
- [23] K. Ariga, A. Vinu, Y. Yamauchi, Q. Ji, J. P. Hill, *Bull. Chem. Soc. Jpn.* **2012**, *85*, 1–32.
- [24] Z. Li, J. C. Barnes, A. Bosoy, J. F. Stoddart, J. I. Zink, *Chem. Soc. Rev.* **2012**, *41*, 2590–2605.
- [25] P. Yang, S. Gai, J. Lin, *Chem. Soc. Rev.* **2012**, *41*, 3679–3698.
- [26] G. P. Dimri, X. Lee, G. Basile, M. Acosta, G. Scott, C. Roskelley, E. E. Medrano, M. Linskens, I. Rubelj, O. Pereira-Smith, M. Peacocke, J. Campisi, *Proc. Natl. Acad. Sci. USA* **1995**, *92*, 9363–9367.
- [27] B. Y. Lee, J. A. Han, J. S. Im, A. Morrone, K. Johung, E. C. Goodwin, W. J. Kleijer, D. DiMaio, E. S. Hwang, *Aging Cell* **2006**, *5*, 187–195.
- [28] M. Knas, A. Zalewska, R. Kretowski, M. Niczyporuk, N. Waszkiewicz, M. Cechowska-Pasko, D. Waszkiel, K. Zwierz, *Folia Histochem. Cytobiol.* **2012**, *50*, 19353.
- [29] B. Lecka-Czernik, E. J. Moerman, R. J. Shmookler Reis, D. A. Lipschitz, *J. Gerontol. Ser. A* **1997**, *52*, B331–B336.
- [30] B. W. Gu, J. M. Fan, M. Bessler, P. J. Mason, *Aging Cell* **2011**, *10*, 338–348.
- [31] S. Chigira, K. Sugita, K. Kita, S. Sugaya, Y. Arase, M. Ichinose, H. Shirasawa, N. Suzuki, *J. Gerontol. Ser. A* **2003**, *58*, B873–B878.
- [32] S. Cabrera, J. El Haskouri, C. Guillem, J. Latorre, A. Beltrán, D. Beltrán, M. D. Marcos, P. Amorós, *Solid State Sci.* **2000**, *2*, 405–420.

- [33] X. Auvray, C. Petipas, R. Anthore, I. Rico-Lattes, A. Lattes, *Langmuir* **1995**, *11*, 433–439.
- [34] R. Perona, R. Machado-Pinilla, C. Manguan, J. Carrillo, *Clin. Trasl. Oncol.* **2009**, *11*, 711–714.
- [35] F. Tang, L. Li, D. Chen, *Adv. Mater.* **2012**, *24*, 1504–1534.
- [36] S. P. Hudson, R. F. Padera, R. Langer, D. S. Kohane, *Biomaterials* **2008**, *29*, 4045–4055.
- [37] A. Bernardos, L. Mondragón, E. Aznar, M. D. Marcos, R. Martínez-Máñez, F. Sancenón, J. Soto, J. M. Barat, E. Pérez-Payá, C. Guillem, P. Amorós, *ACS Nano* **2010**, *4*, 6353–6368.
-